EM-PIC SIMULATIONS OF e-BEAM INTERACTION WITH FIELD EMITTED IONS FROM BREMSSTRAHLUNG TARGETS*

P. W. Rambo and S. Brandon
Lawrence Livermore National Laboratory, Livermore CA 94550

Abstract

We investigate electron beam defocusing caused by field emitted ions from the bremsstrahlung target of a radiography machine using fully electromagnetic particle-in-cell simulations. This possibly deleterious effect is relevant to both current radiography machines (FXR) and machines being built (DARHT-2) or planned (AHF). A simple theory of the acceleration of ions desorbed from the heated target, and subsequent beam defocusing due to partial charge neutralization is in reasonable agreement with the more detailed simulations. For parameters corresponding to FXR (I_b=2.3 kA, ε_b=16 MeV), simulations assuming space-charge-limited emission of protons predict prompt beam defocusing. Time integrated spot-size measurement, however, is dominated by early-time small spot brightness, and so is not a sensitive diagnostic. Comparisons are made to available FXR data. We also investigate use of a recessed target geometry to mitigate field emitted ion acceleration; only modest improvements are predicted.

1 INTRODUCTION

Current radiography machines such as FXR, as well as future machines such as DARHT-2 and the proposed Advanced Hydrodynamic Facility (AHF), make use of an intense electron beam striking a high-Z target to generate high-energy bremsstrahlung radiation. It is necessary that the electron beam be focused to a small spot for good radiographic definition. In FXR and DARHT-2, and the proposed AHF machine, the beam is created in a linear induction accelerator (LIA), and is focused in a low applied-field drift region. Dale Welch [1] at MRC first identified a potential problem due to ion field emission for DARHT–2, arguing that target heating from the beam would quickly provide a source of ions which can be accelerated by the beam space-charge, and back stream toward the beam source. The excess charge neutralization then causes the beam to pinch, and subsequently defocus.We describe results from electromagnetic PIC simulations for FXR parameters, which predict prompt defocusing for space-charge-limited proton emission. Comparison to available experimental data suggests that the emission onset is substantially delayed in time or reduced from the space-charge-limit, if not absent entirely.

2 SPACE CHARGE LIMITED EMISSION AND BEAM DEFOCUSING

Welch has argued that once the target surface is heated beyond 400 °C, impurities are readily desorbed and ionized. These impurities, including both protons and carbon ions, are then free to be accelerated by the beam space charge potential. Nominally, FXR operates at a total current of $I_b \approx 2.3$ kA focused to a spot size of $r_b \approx 0.1$ cm; thus the current density is approximately $J_b \approx 70$ kA/cm^2 and particle flux $J_b/e = 5\times10^{23}$ /cm$^2\cdot$s. At the beam energy ε_b =16 MeV, ionization energy loss in Ta is $d\varepsilon/dx \approx 20$ MeV/cm at solid density, and the average energy increase per atom is approximately 0.2 eV/ns. Thus the target is very quickly heated, and any surface contaminants are expected to be available for ionization and subsequent acceleration.

A simple theory serves to estimate the properties of these emitted ions and their interaction with the electron beam; units are Gaussian, except where results in more convenient units are specifically indicated. Approximate the beam as a cylinder of radius r_b with uniform density n_b, both corresponding to the target focus. The beam is traveling at nearly the speed of light, c, with relativistic factor γ_b. The potential difference between the center of the beam and its edge, as well as the (radial) electric field are easily calculated; the axial field at the target will be approximately the same,

$$\Phi_b \approx \pi e n_b r_b^2 \approx I_b / c\,; \quad E_z \approx E_r = 2\Phi_b / r_b\,. \qquad (1)$$

For FXR parameters, this predicts an electric field at the target surface of order $E_z \approx 1.4$ MeV/cm. The current of emitted ions (mass $M_i = A_i m_p$ and charge $q_i = Z_i e$, with m_p the proton mass) may be estimated using the well known result for Child-Langmuir space-charge-limited current. Using the beam potential just estimated and a distance equal to the beam radius,

$$J_i \approx \frac{\left(2q_i / M_i\right)^{1/2} \Phi_b^{3/2}}{9\pi r_b^2}\,; \quad I_i \equiv \pi r_b^2 J_i\,, \qquad (2)$$

which predicts an emitted ion current $I_i/I_b \approx 0.2\%$ for FXR. The ions are quickly accelerated to an energy of the order of the beam potential, and hence velocity $v_i = (2q_i\Phi_b/M_i)^{1/2}$. The ion density is then estimated from $n_i = J_i/v_i q_i$, showing the surprising result that the charge neutralization fraction f is a constant: $f \approx 1/9$. The contribution to the radial field from this ion charge is equal to the field generated by the beam decreased by the factor f, $E_+ = fE_r$. In a time τ, the ions will move a length $L \approx \tau v_i$ and beam electrons will be radially accelerated as they traverse this distance to the target, $t \approx L/c$. Equating the radial deflection to the beam radius gives an estimate for the time τ required to defocus the beam,

$$\delta r \approx \frac{1}{2}\frac{eE_+}{\gamma_b m_e}t^2 \approx \frac{1}{2}\frac{e}{\gamma_b m_e}\left(f\frac{2\Phi_b}{r_b}\right)\left(\frac{\tau v_i}{c}\right)^2 \equiv r_b\,, \qquad (3)$$

$$\tau \approx 5ns\,\frac{r_b(mm)}{I_b(kA)}\sqrt{\frac{\gamma_b A_i}{Z_i}}\,.$$

* This work was performed under the auspices of the U. S. Department of Energy by Lawrence Livermore National Laboratory under contract No. W-7405-Eng-48

For FXR parameters, this theory predicts a time to defocus of $\tau \approx 10$ ns for proton emission, well within the pulse time of 60 ns. Of course this theory is quite simplified; we next turn to self consistent simulations.

3 EM-PIC SIMULATIONS

Direct particle-in-cell (PIC) simulation of intense beams has a long and successful history, both at LLNL and elsewhere. We have simulated ion emission and subsequent beam defocusing with both CONDOR, a well-tested design code developed over many years within A-division, and a new code, CODA, that allows non-rectangular zones. Both codes are fully relativistic, 2-1/2 dimensional (2-spatial dimensions in axisymmetric *Z-R* geometry, 3-velocity dimensions) electromagnetic (EM) PIC codes. The simulation geometry is a cylinder of radius 4 cm and length 25 cm with conducting boundaries. The beam is injected at the left hand boundary with an initial radius of 2.0 cm, and with uniform current density. The beam is injected with finite emittance so as to be focused at the target; no externally applied fields are present. The injected beam current is linearly ramped up in 10 ns, constant for 40 ns, then linearly ramped down again in 10 ns. The right hand end-plate forms the absorbing target, from which ions are emitted. No modeling of the target heating or surface physics is included; the space-charge-limited emission is simply turned on at a preselected time, over a specified radial region. Simulations presented here were all performed with CODA utilizing a converging mesh that allows much better resolution at the target surface, $\Delta r = 200$ μm and $\Delta z = 600$ μm.

The time history of the RMS beam radius at the target is shown in Fig. 1 from a typical simulation. The injected beam is characteristic of FXR, with $I_b = 2.3$ kA, $\varepsilon_b = 16$ MeV ($\gamma_b \approx 32$) and initially focused to a root-mean squared (RMS) radius $r_b = 0.06$ cm. Proton emission is turned on at t=15 ns, in the region $0 < r < 0.06$ cm. The initial pinch and subsequent defocus occur very quickly in

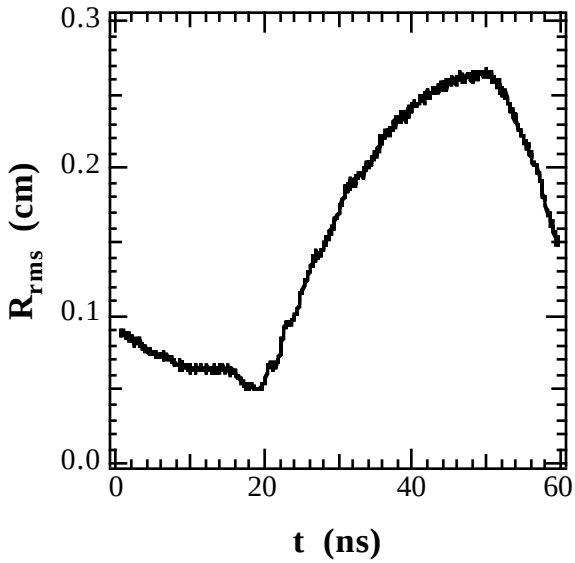

Fig. 1 Time dependent beam radius at target from a simulation of FXR with proton emission turned on at t=15ns.

agreement with our previous estimate. As the beam defocuses, emission decreases (from a peak of $I_i \approx 8$ A) because of the reduced electric field at the emission area. Many aspects of the simple theory previously developed are observed in these simulations, namely the magnitude of the axial electric field at the target surface, the time for pinching to occur, and the small ratio of emitted ion current to beam current (<1%). The scaling of the time to defocus, Eq. (3), with ion mass and beam current has also been confirmed by additional simulations. An important observation is that the total number of field emitted ions, N_i, is quite small: for this simulation $N_i = 5.7 \times 10^{11}$ at t=30 ns. This corresponds to a fraction of approximately 10^{-4} from a monolayer of equal area, suggesting that surface cleaning would be a very difficult proposition.

4 COMPARISON WITH FXR DATA

We now consider available data from FXR. Two principle measurements are used to assess spot quality at FXR; both are time-integrated radiographic measurements. The first uses an opaque "roll bar" to cast a shadow from the bremsstrahlung spot; the width of the edge of this shadow reflects the finite spot size. Careful unfolding of the data shows a central peak with FWHM spot size of 1.1mm, surrounded by a low density "halo" with relative brightness of a few percent of the central peak [2]. In the second measurement, forward bremsstrahlung dose is measured both with and without an 800 μm diameter collimator. The collimated dose is observed to be approximately 1/3 of the forward dose in the absence of the collimator; this is observed to be the case both for beam currents of 2.3 kA and 3.3 kA [3].

Although the experimentally observed small spot seems at odds with the defocusing seen in the simulations, e.g. Fig. 1, this is not necessarily so. Because the beam density at the target is inversely proportional to the square of the spot size, $n_b \propto I/r^2$, the bremsstrahlung emission from the defocused beam is very dim and a time integrated measurement can be dominated by the early-time small spot brightness. In Figure 2, we show the time integrated beam density at the target (normalized) as a function of radius from the simulation illustrated in Fig. 1. As can be seen, the contribution from the defocused beam is a low density halo. The level of the halo relative to the central peak is determined by the relative duration of the focused and unfocused periods of the time history. This is illustrated in Fig. 2, which also shows results from simulations with the ion emission turned on at 10 and 30 ns. The level of the halo is also affected by the defocused radius; allowing ion emission from a larger area increases the defocused beam spot, decreasing the relative beam density in the halo.

We next consider the collimated dose measurements. The angular spectrum of bremsstrahlung photons created by 16 MeV electrons striking a 1mm thick Ta target was calculated using a Monte Carlo code [4]; this angular spectrum is then used to determine the contribution to the forward dose from each simulation electron as it strikes the target. Figure 3 shows the time dependent forward

dose (normalized) for the simulation shown in Fig. 1. Because the electrons strike the target with larger angles

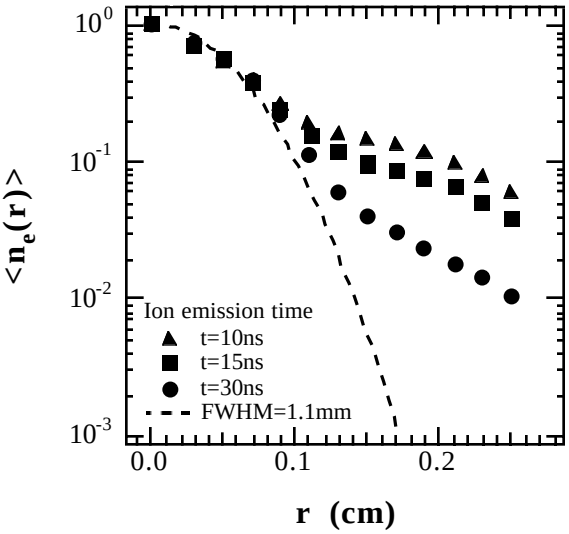

Fig. 2 Time averaged beam density at target from FXR simulations including proton emission; three different emission onset times are shown.

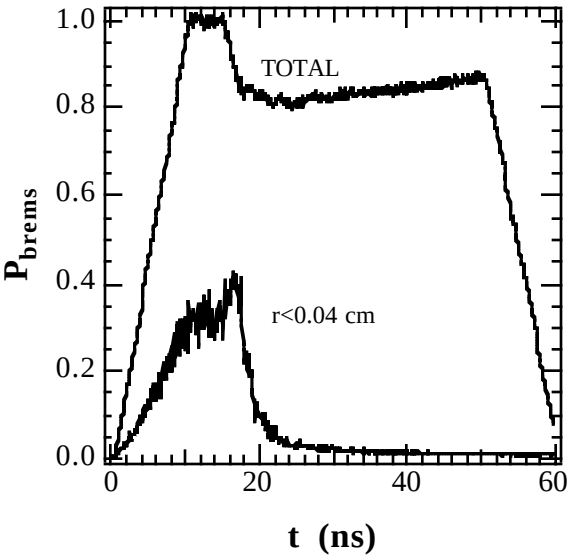

Fig. 3 Time dependent forward dose from FXR simulation including proton emission for t>15 ns.

after pinching, the total forward dose decreases approximately 20%. More importantly, however, the forward dose from electrons striking the target with r<400 μm is abruptly cut-off as the spot size increases. For this case the time integrated forward dose from electrons entering the target with r<400 μm is 0.14 of the total calculated forward dose. Again, this fraction varies with the onset time for ion emission; for onset times of 10 ns and 30 ns (see Fig. 2) the forward dose fractions are 0.10 and 0.23 respectively. With the beam current increased to I_b=3.3 kA, similar results are obtained except that the forward dose fraction is further decreased: for proton emission onset times of 15 ns and 30 ns the forward dose fractions are 0.11 and 0.20 respectively. The forward dose fraction for these simulations in the absence of ion emission is 0.30. Decreasing the focused beam radius to r_{RMS}= 0.05 cm (by decreasing the injection emittance) increases the unperturbed fractional transmission to 0.40; for this focus and I_b=3.3 kA, proton emission turned on at t=30 ns decreases the time integrated fractional forward dose to 0.26. Further decrease of the focused beam radius would be in disagreement with the spot size measurements.

Simulations were also performed with singly ionized carbon emission for comparison. Turning on C^+ emission at t=15ns for the I_b=3.3 kA case gives a forward dose fraction of 0.20 due to the slower defocusing, still significantly less than observed; delaying the C^+ emission until t=30 ns results in a forward dose fraction of 0.28.

5 DISCUSSION

We have seen from simulations with parameters relevant to FXR, that beam defocusing occurs quickly after the onset of proton emission. Time integrated spot size measurements are not a sensitive measure of defocusing, however, because the defocused beam only contributes a dim halo compared to the central peak from the small spot emission. But the level of the halo, observed to be a few percent relative to the central peak in FXR measurements, does rule out prompt proton emission, t<15 ns. The collimated dose is a more stringent test. Proton emission beginning at time earlier than t≈30 ns is inconsistent with the observation that one third of the forward dose is transmitted through an 800 μm collimator. Bounds on the emission of singly ionized carbon are only slightly less restrictive.

The simplest explanation is that ion emission is not occurring on FXR, or at currents reduced far below the space charge limit (approximately a factor of 30 decrease is necessary). This does not preclude a disastrous effect on machines with higher current densities, however, since there may still be a threshold for ion formation. Because of this, methods to minimize this effect are being pursued. In particular, we have simulated the effect of recessing the target so as to reduce the emitted ion current. Although the time for defocusing is increased, and the defocused beam spot size decreased, this still does not appear to be satisfactory. Used in conjunction with other means for isolating the emitted ions, however, might be acceptable. We look forward to experimental results from ETA-II (to be reported at this conference), including time resolved measurements that may give a more definitive answer concerning these effects.

ACKNOWLEDGMENTS

The authors wish to acknowledge numerous useful discussions with Y.-J. Chen, G. Caporaso, N. Back, R. Scarpetti, M. Aufderheide, D. Ho, and P. Bergstrom.

REFERENCES

[1] D. R. Welch, "Effects of electron-ion streaming due to beam-target interactions," presented at the DARHT-2 Review (January 16, 1997).
[2] N. Back, internal memorandum (March 24, 1997).
[3] R. Scarpetti, private communication (May 14, 1998).
[4] P. Bergstrom, private communication (October 3, 1997).